香港浸會大學
HONG KONG BAPTIST UNIVERSITY

HKBU Scholars

Probing Bulk Transport, Interfacial Disorders, and Molecular Orientations of Amorphous Semiconductors in a Thin-Film Transistor Configuration

Sit, Wai Yu; Cheung, Sin Hang; Chan, Cyrus Yiu Him; Tsung, Ka Kin; Tsang, Sai Wing; So, Shu Kong

Published in:
Advanced Electronic Materials

DOI:
10.1002/aelm.201500273

Published: 01/03/2016

Document Version:
Peer reviewed version

Link to publication

Citation for published version (APA):
Sit, W. Y., Cheung, S. H., Chan, C. Y. H., Tsung, K. K., Tsang, S. W., & So, S. K. (2016). Probing Bulk Transport, Interfacial Disorders, and Molecular Orientations of Amorphous Semiconductors in a Thin-Film Transistor Configuration. *Advanced Electronic Materials*, *2*(3), Article 1500273. https://doi.org/10.1002/aelm.201500273

General rights
Copyright and intellectual property rights for the publications made accessible in HKBU Scholars are retained by the authors and/or other copyright owners. In addition to the restrictions prescribed by the Copyright Ordinance of Hong Kong, all users and readers must also observe the following terms of use:

- Users may download and print one copy of any publication from HKBU Scholars for the purpose of private study or research
- Users cannot further distribute the material or use it for any profit-making activity or commercial gain
- To share publications in HKBU Scholars with others, users are welcome to freely distribute the permanent publication URLs

Downloaded on: 27 Apr, 2025

Authors
Wai-Yu Sit, Sin Hang Cheung, Cyrus Yiu Him Chan, Ka Kin Tsung, Sai Wing Tsang, and Shu Kong So

This journal article is available at HKBU Institutional Repository: https://repository.hkbu.edu.hk/phys_ja/213

DOI:
Article type: Full Paper

Title: Probing bulk transport, interfacial disorders, and molecular orientations of amorphous semiconductors in a thin-film transistor configuration

*Wai-Yu Sit, Sin Hang Cheung, Cyrus Yiu Him Chan, Ka Kin Tsung, Sai Wing Tsang, and Shu Kong So**

Wai-Yu Sit, Sin Hang Cheung, Cyrus Yiu Him Chan, Ka Kin Tsung, Prof. S. K. So
Department of Physics and Institute of Advanced Materials,
Hong Kong Baptist University,
Kowloon Tong, Hong Kong,
P. R. China
E-mail: skso@hkbu.edu.hk

Prof. S. W. Tsang
Department of Physics and Materials Science,
City University of Hong Kong,
Kowloon Tong, Hong Kong,
P. R. China

Keywords: (Charge transport, Molecular orientation, Organic thin film transistors, Time-of-flight, Organic light emitting diodes)

Abstract

Thin film transistors (TFTs) can be used to determine the bulk-like mobilities of amorphous semiconductors. Different amine-based organic hole transporting materials (HTs) used in organic light-emitting diodes (OLEDs) have been investigated. In addition, we also measure the TFT hole mobilities of two iridium phosphors: $Ir(ppy)_3$ and $Ir(piq)_3$.

These materials were grown separately on SiO_2 and polystyrene (PS). On SiO_2, the TFT mobilities are found to be 1-2 orders smaller than the bulk values obtained by time-of-flight (TOF) technique. On PS gate dielectric layer, the TFT mobilities are in good agreement TOF data. Only 10 nm of organic semiconductor is sufficient for TFTs to achieve TOF mobilities. Using the Gaussian Disorder Model (GDM), we found that on SiO_2 surface, when compared to the bulk values, the energetic disorders (σ) of the HTs increase and simultaneously, the high temperature limits (μ_∞) of the carrier mobilities decrease. Both σ and μ_∞ contribute to the reduction of the carrier mobility. The increase in σ is related to the presence of randomly oriented polar Si-O bonds. The reduction of μ_∞ on SiO_2 is related to the orientations of the more planar molecules which tend to lie horizontally on the surface.

1. Introduction

Organic semiconductors (OSCs) are now widely used in optoelectronic devices. [1-6] So far, organic light-emitting diodes have been the most successful for device applications. Many commercial products are now available. [7-9] It is well known that the charge-carrier mobility is one of the key parameters to determine the device efficiency, not only for balancing the charges for higher quantum efficiency, but also for engineering the emission zone to achieve a suitable emission spectrum.[10-11] Different methods have

been employed to probe the mobilities including as time-of-flight (TOF) technique,[12-13] CELIV, DI, organic thin-film transistors (OTFTs),[14-18] admittance spectroscopy[19] and current-voltage measurements.[20] Among all the techniques, TOF is probably the most reliable because it is model-free and does not require Ohmic injection contacts. However, the material consumption for TOF is very high, because a thick organic film of several μm thickness is required. So TOF is not practical especially for newly synthesized materials with small quantities.

To reduce material consumption for carrier transport characterization, various schemes have been attempted. Qiu et. al. measured carrier mobilities of amorphous hole transporters in a device using a transient voltage excitations. The carrier transit times were deduced from the falling-edge transient of the output current.[21] The organic layer under investigation has a thickness of between 100-200 nm, but a special device needs to be constructed. More recently, Liu et. al. introduced a modified TOF with a charge-generation layer (CGL). [22] The CGL consists of SuPc doped with CuPc that strong strongly absorbs at visible light, and acts as a charge injection layer for the incoming laser for TOF. With the new CGL, the sample thicknesses for TOF experiment can be reduced to about 300 nm.

Below, we describe a low-material-consumption approach of measuring bulk carrier

transport of amorphous organic semiconductors and found that organic thin film transistor (TFT) technique can serve such a purpose. The bulk/TOF mobilities of amine-based hole transporters (HTs) that are commonly used in OLED devices can be evaluated when polystyrene (PS) is employed as the gate dielectric layer in organic TFTs. In contrast to a PS gate dielectric layer, TFT mobilities are 1-2 orders lower than the bulk values for organic semiconductors grown on SiO_2.[23] Temperature dependent measurements were carried out to examine the origins of reduced mobilities. It can be shown on SiO_2 surface, the energetic disorders (σ) of the HTs increased. Simultaneously, the high temperature limits (μ_∞) of the carrier mobilities decreased. Both σ and μ_∞ contribute to the reduction of the carrier mobility. The increase in σ is related to the presence of randomly oriented polar Si-O bonds. The reduction of μ_∞ is topological in origin and is related to the orientations of the more planar molecules on SiO_2 as revealed by an analysis of the initial growth of molecules on SiO_2 and PS surfaces. The results are further supported by comparing TFT mobilities obtained in two 3-dimensional iridium phosphors.

2. Results and discussion

2.1 Achieving bulk mobility in TFT configuration

Figure S1 shows the chemical structures and the HOMO values of the four HTs,

N,N'-Di(1-naphthyl)-N,N'-diphenyl-(1,1'-biphenyl)-4,4'-diamine(NPB),4,4',4''-Tris[2-naphthyl(phenyl)amino]triphenylamine(2TNATA),N,N'-Bis(3-methylphenyl)-N,N'-diphenylbenzidine (TPD), and N,N'-bis(3-methylphenyl)-N,N'-bis(phenyl)-9,9-spirobifluorene (Spiro-TPD). The TFT mobilities in the linear (μ_{lin}) and saturation (μ_{sat}) regions were evaluated by standard equations [19]:

$$I_{ds} = \frac{W}{L}\mu_{lin}C_i(V_g - V_t)V_{ds} \quad (1)$$

$$I_{ds} = \frac{W}{2L}\mu_{sat}C_i(V_g - V_t)^2 \quad (2)$$

where I_{ds} is the source-to-drain current, W is the channel width, L is the channel length, C_i is the capacitance of the gate dielectric per unit area; V_{ds} , V_g and V_t are the applied source to drain voltage, the gate voltage, and the threshold voltage of the OTFT respectively. The TFT output characteristics of NPB on PS and NPB on SiO_2 are shown in **Figure 1**. The output currents for the NPB transistors varied from 0-20nA on SiO_2. On the other hand, the output currents increased to the range of 0-400nA when NPB was grown on PS. The results indicate the output currents are much more favorable for the NPB grown on PS. Besides, NPB similar experiments have been conducted on other hole transporters, TPD, Spiro-TPD, and 2TNATA. The transfer characteristics are shown in **Figure 2**. The results show that all the amine-based compounds have improved output currents on PS. The measured TFT mobilities in the linear and saturation regions for all amine-based

compound are summarized in **Figure 3**. Table S1 in the Supplementary Information provides further device characteristics including the threshold voltages and on/off ratios. We can see for all amine compounds, the TFT mobilities on SiO_2 are consistently lower than the TFT mobilities on PS gate dielectric. In Figure 3, we also show the hole mobilities of all amine compounds (dashed line) as measured independently by time-of-flight (TOF) technique at low electric field. It can be seen that the TOF mobilities are essentially the same as the TFT mobilities on PS. Thus we conclude that, from a metrological point of view, TOF mobility, which is a measure of the bulk carrier transport of the HTs, can be achievable in a TFT configuration but with much reduced film thicknesses.

2.2 Thickness dependence measurements

To check how much organic material is needed for TFT characterization of carrier mobility, we chose NPB as the reference material, and performed a detailed thickness dependent measurement on its hole mobilities on both SiO_2 and on PS. **Figure 4** presents the thickness dependent results. We first focus on the data using PS gate dielectric layer. Above 10 nm, the TFT mobility is essentially constant and independent of the thickness of the organic layer. The values are between 4 - 6×10^{-4} cm^2/Vs. The horizontal blue color band in the mobility plot represents the bulk mobility region obtained from TOF. After

employing PS as gate dielectric layer in TFT configuration, one can achieve bulk mobility even when the thickness of the organic layer is down to 10 nm. The result here should be contrasted with TOF results in which a much thicker film (typical 100 times thicker) is required. For those TFTs with NPB thicknesses below 10 nm, the mobility drops rapidly as thickness is further reduced, and no reliable mobility can be obtained below 5 nm. Dinelli proposed phenomenological model to characterize the thickness dependent TFT mobility with:[24]

$$\mu = \mu_s (1 - e^{[-(\frac{d}{d_0})^{\alpha}]}) \quad (3)$$

where μ is the mobility of the organic semiconductor, μ_s is the saturation mobility of the organic semiconductor (when the film is thick enough), d is the film thickness, d_o is the critical thickness required to obtain a reliable mobility value, and α is the exponent parameter to represent the quality of the charge conduction. Using Equation 3, we fitted the data, and obtained a d_0 of 7.6 nm.

In Figure 4, we also show the TFT mobilities of NPB grown on SiO_2. The overall thickness dependence in this case is very similar to the case on PS, except that the data on SiO_2 are about one and a half order smaller. The hole mobility levels off when the film thickness exceed 10 nm. Increasing the thickness of NPB to 100 nm does not help to

improve the mobility further. The results on SiO_2 confirm the notion that in a TFT, the transport of charge carriers occurs within a few layers above the gate dielectric layer. (If charge transport were to involve layers well above the gate dielectric, the bulk value of μ should be achievable for NPB grown on SiO_2). The mobility saturation thickness can be further correlated with the growth of well-connected NPB molecules near the gate dielectric. AFM data (from Fig. 6) show that NPB molecules form discrete islands between 3-5 nm. Large amount of voids are present below this range of thickness. Above 5nm, the NPB islands start to percolate as indicated by detectable TFT signals in Fig. 4. Additional NPB molecules are needed to eventually fill these voids. The thickness dependent TFT data suggests that percolation completes when a total nominal film thickness of 10 nm is reached. Despite the similarities in the thickness dependences on PS and SiO_2, the transport of holes above SiO_2 is distinctly lower. Below we will examine the origins of the reduced mobilities on SiO_2.

2.3 Temperature dependence transport measurements of organic films on SiO_2 and PS gate dielectric layers.

To look into the origins of different TFT mobilities on SiO_2 and on PS, temperature dependence TFT measurements were performed between 235K and 351K. The extracted hole mobilities were analyzed by the well-known Gaussian Disorder model (GDM).[25] In

the GDM, the mobilities are electric field (F) and temperature (T) dependent.

$$\mu(F,T) = \mu_\infty \exp\left[-\left(\frac{2\sigma}{3k_BT}\right)^2\right]\exp\left(\beta F^{\frac{1}{2}}\right) \quad (4)$$

where k_B is the Boltzmann constant, μ_∞ is the high temperature limit of the mobility, and

$$\beta = C\left[(\frac{\sigma}{k_BT})^2 - \Sigma^2)\right] \quad (5)$$

β is the Poole-Frenkel slope and C is a fitting constant. The charge carriers experience an energetic disorder (σ) and positional disorder (Σ) which can be understood as the width of the Gaussian distribution of the energy states and the positional/orientational fluctuations of the transport sites, respectively. At low field ($F \rightarrow 0$), the second exponential term in Equation 4 approaches 1 and $\mu(0,T) \sim \exp\left[\frac{4}{9}(\frac{\sigma}{k_BT})^2\right]$. A semi-log plot of low field mobilities (using μ_{lin}) versus $1/T^2$ should yield a straight line. σ and μ_∞ can be extracted from the slope and y-intercept of the line, respectively.

Figure 5 shows the temperature dependent TFT-derived mobilities data for all the four amine-based compounds analyzed by the GDM model. In addition, we also show hole mobility data obtained independently by TOF experiments. Several features can be noted. First, there are excellent agreements between the TFT data on PS and the TOF

results at all temperatures. This observation substantiates that the bulk-like transport behavior from TOF can be realized in a TFT structure. Thus, TFT can be considered to be a low material consumption approach to evaluate bulk-like mobility of an organic semiconductor. Second, for all organic semiconductors shown in Figure 5, TFT data on SiO_2 possess distinctly steeper slopes when compared to TFT data on PS. According to Equation 4, the energetic disorders can be evaluated from these slopes and the results are summarized on Table 1. On PS, the energetic disorders σ are in the narrow range between 71-77 meV, and the values are very similar to that obtained from TOF.[33] On the other hand, σ are much larger when the organic semiconductors are grown on SiO_2. A model, which is consistent with observed increase in σ, can be attributed to the presence of randomly oriented dipoles associated with polar Si-O bonds on the thermally grown SiO_2 surface.[23,26] These random dipoles broaden the density-of-states of the charge hopping manifold, and increase σ. In contrast to SiO_2 surface, PS is non-polar. As a result, holes (once injected from the source electrode) only experience the intrinsic energetic disorder, which is very similar to the environment encountered in a TOF configuration.

Besides differences in the energetic disorder parameters, we also note from Figure 5 that TFT data on SiO_2 surfaced possess reduced μ_∞ for all organic semiconductors when compared to the TFT data obtained on PS. Table 1 summarized the μ_∞ data obtained from

both gate dielectric surfaces. Following the concept of the GDM, μ_∞ is related to the hopping rate across the neighboring transporting sites. The rate can be described by: [27]

$$\mu_\infty = \frac{\nu_0 a^2 e}{\sigma}\exp(-2\gamma a) \tag{6}$$

where v_0 is the attempt-to-hop frequency, a is the average hopping distance, e is the elementary charge, and γ is the inverse localization radius. γ is primarily determined by the active site for charging hopping. In Figure 5, all compounds are amine-based and the amine moieties are the electron donating sites. So γ can be taken as a constant. Therefore, for a given organic semiconductor shown in Figure 5, the difference in μ_∞ can only arise from a difference in the effective hopping distance a. The results from Figure 5 suggest that the average charge hopping distance on SiO_2 surface is larger than that of PS surface. Therefore, using Equation 6 and assume $\nu_0=10^{14}$ Hz in an order of phonon frequency,[28] we can compute a and the results are shown in Table 2. Summarizing the temperature dependence experiments, we conclude that the TFT mobilities on SiO_2 surface are reduced compared to the data on PS. Two factors give rise to the reduced mobilities. The first factor is energetic in origin which is attributed to the randomly oriented polar Si-O bonds on the oxide surface. The second factor is related to the charge hopping distance. As we see below, the latter factor is topological in origin and is closely correlated to the orientation of the organic molecules right above the gate dielectric layer.

2.4 Morphology study on organic thin films

To check if the difference in μ_∞ is related to the morphologies of the organic films, we use NPB as an example, and took a series of AFM images for different thicknesses of NPB on SiO_2 and PS. Special attention is given to the initial growth of the NPB films on the two different surfaces. **Figure 6** shows the images for nominal NPB thicknesses between 0-5 nm. First, the bare surfaces of SiO_2 and PS are generally smooth and the roughnesses are less than 0.2 nm. On the PS surface, between a nominal thickness between 1.5 and 3 nm, NPB molecules form discrete islands. These islands are roughly circular or oval in shapes and are quite homogeneous. They grow in sizes until they start to percolate at around 5 nm. The growth of NPB on PS is consistent with the thickness dependent TFT measurements shown in Figure 4 in which we observed negligible mobilities below a film thickness of 5 nm on PS. The thin film of NPB on PS percolates at about 5 nm. For thicker NPB film, we expect in relation to the substrate, the molecular orientation of an NPB molecule is random on PS. This kind of orientation mimics the bulk. Therefore, one can obtain the bulk mobility (TOF mobility) when well-connected NPB molecules are deposited on PS.

In contrast to PS, the growth of NPB on SiO_2 is very different. On SiO_2 surface,

NPB molecules form discrete islands between 1.5 and 3 nm. But the islands are larger and their shapes are more irregular. Compared to the islands on PS surface, these NPB islands on SiO_2 have much larger lateral dimensions, suggesting that NPB molecules interact much stronger with SiO_2 than with PS. The interaction between NPB molecule and the surface would favor a configuration in which the molecule prefers to orient itself parallel (horizontal) to the surface, with their π-orbitals facing down. As the NPB film grows from 1.5 to 3 nm, the roughness of the film significantly reduces from 2.2 nm to 0.9 nm. At the same time, most of the voids between the islands disappear, indicating that fresh incoming molecules prefer to sit on bare SiO_2 regions, consistent with a model in which NPB orients horizontally with respect to the surface. In fact, recent experimental and computational studies support our observations. From ellipsometry measurements, it was shown that linear amorphous molecules like NPB are oriented on glass, with their long axes lie in the plane of the substrate. [29-31]

Figure 7 shows a model for the molecular orientations of NPB on SiO_2 and PS. On SiO_2, as NPB molecules prefer to lie horizontally on the surface, their π orbitals would be perpendicular to the surface, which is not favorable for charge transport along the surface in TFT configuration. This will result in an effective increase in the average charge hopping distance a, reduced μ_∞, and reduced carrier mobility even when the energetic

disorder contribution is negligible at high temperatures as suggested by Equation 4. Besides NPB, other molecules that can adopt planar conformations are expected to behave in very similar manners on SiO_2 surface. We conclude that on SiO_2 surface, molecules that have planar conformations tend to lie horizontally with respect to the substrate when the substrate temperature is lower than T_g. Such an orientation will lead to poor π-π overlaps and is unfavorable for charge transport parallel to the surface and suppress the TFT hole mobility of these molecular films. On the other hand, when PS is used as the gate dielectric layer, these molecules orient themselves randomly as shown in Figure 7. This kind of growth mimics the bulk-like orientations and results in a carrier mobility similar to TOF mobility. For NPB, TPD, and 2TNATA, they all possess planar conformations in which they can interact with the polar SiO_2 surface, adopt horizontal orientations, and results in reduced μ_∞. In all three cases, the reduction in μ_∞ is 25% to 35% of the bulk value of about 2×10^{-2} cm^2 V^{-1}s^{-1}. However, due to the presence of the spiro core, spiro-TPD possesses a 3-D structure, which is less influenced by the polar nature of SiO_2 gate dielectric. The two amine moieties can still orient horizontally, but now the two phenyl rings linking the amines groups are lifted up. So we anticipate a weaker interaction between spiro-TPD and SiO_2, and the reduction of μ_∞ should not be as large as the other planar compounds. In fact, μ_∞ obtained on both gate dielectric has little

difference, as indicated from the nearly overlapping y-intercepts in Figure 5 for spiro-TPD.

2.5 Morphology and transport studies on 3D molecules

In the last section, we show that the difference in mobility between SiO_2 surface and PS surface partially originates from the planar conformations of NPB, TPD, and 2TNATA. To substantiate our conclusion, we introduce two non-planar molecules, $Ir(ppy)_3$ and $Ir(piq)_3$. The HOMO energy levels and chemical structures of the iridium compounds are shown in Figure S1. We performed TFT measurements for both $Ir(ppy)_3$ and $Ir(piq)_3$ on SiO_2 and PS. The molecular structure of $Ir(piq)_3$ is shown in Figure S1 and the transfer characteristics of $Ir(piq)_3$ and NPB on PS and SiO_2 are shown in **Figure 8**. The difference in output currents of NPB on both surfaces has more than one order in magnitudes. However, using a 3-D molecule, $Ir(piq)_3$, the output currents on both surfaces have no significant changes. We expect the non-planar conformation of $Ir(piq)_3$ leads to similar output currents. Since $Ir(piq)_3$ is a 3-D molecule, the π-π overlap between the molecules are similar no matter how the molecules are grown on SiO_2 or PS. Therefore, the output currents of $Ir(piq)_3$ on both surfaces are similar. Besides $Ir(piq)_3$, we also measured the hole mobilities of $Ir(ppy)_3$ and similar conclusions can be drawn as in the case of $Ir(piq)_3$.**Figure S2** shows the temperature dependent measurements of $Ir(ppy)_3$

and $Ir(piq)_3$ on PS and SiO_2. The results are consistent with Figure 8. The hole mobilities of $Ir(ppy)_3$ and $Ir(piq)_3$ show insignificant changes on SiO_2 or PS.

Finally, we wish to comment on the limitations of our approach for evaluating carrier mobility. First, the data we have presented are only confined to HT compounds. In fact, the concepts should work for both electron and hole transporting materials. In reality, electron mobility is much more difficult to measure. It is known that residual moisture and/or O_2 introduce trap levels below the LUMO level of most n-type OLED materials.[32] These traps are known to hinder electron transport, making reliable electron mobility determination very difficult in both TOF and TFT experiments. Second, we note that TFT technique can only be used to probe bulk-like mobilities when the organic film is amorphous and isotropic. In the case of a non-interacting gate dielectric layer (e.g. PS), the amorphous nature of the film is retained, and the environment should mimic the bulk. So, bulk-like carrier mobility can be obtained as in TOF. Supporting evidences for the bulk-like environments for hole transports on TFTs with a PS gate dielectric layer are the nearly identical energetic disorder parameters shown in Table 1. Third, our results suggest that molecules that can adopt more planar conformations will be prone to stronger interaction with the gate dielectric, resulting in reduced mobilities. In contrast, those with more 3D structures will be more favorable for mobility evaluations with a TFT structure.

3. Conclusions

Our findings can be summarized in two aspects. First, we show that organic TFT can be used as a tool of metrology for probing bulk transport properties of organic semiconductors. To do this, the gate dielectric layer for the TFT structure needs to be non-polar. The non-polar surface can be realized through deposition of non-polar polymer or organic insulator. On such a surface, we observe bulk-like transport behaviors for amorphous organic semiconductors. The thickness of the organic layer required is down to about 10 nm — less than 1% of the TOF consumption. Second, we point out that the TFT can also serve as a tool to study gate dielectric / organic interactions. Through temperature dependent measurements, interfacial energetic disorders can be evaluated using an organic semiconductor with known intrinsic transport properties. Furthermore, the high temperature limits of the carrier mobilities can be correlated with the orientations of the molecules with a planar conformation. Our findings signify a key advance in the transport characterization of organic semiconductors and should be of general interest to the research community.

4 Experimental Details

NPB, Spiro-TPD, 2TNATA, TPD, $Ir(piq)_3$ and $Ir(ppy)_3$ were purchased from e-Ray Optoelectronics Technology Co., Ltd. Figure S1 shows the chemical structures and the HOMO values of the four HTs, as well as $Ir(ppy)_3$ and $Ir(piq)_3$. All materials were used as received. MoO_3 was purchased from Strem Chemicals, Inc. Polystyrene (PS) was purchased from Sigma Aldrich. Co.. Heavily doped p^+-silicon substrates were thermally grown with 300 nm of SiO_2. Before device fabrication, the substrates were cleaned by deionized water, filtered acetone and iso-propanol with 20 minutes each. After 13 minutes of UV-Ozone treatment, PS was dissolved in 1,1,2-trichloroethane at a concentration of 6.5 mg/ml and spun on the silicon substrate at 2000 rpm for 1 minute. The substrates were then stored in a vacuum oven at 60 ℃ for 12 hours to remove any unwanted solvents. Both SiO_2 and PS surfaces possess smooth surfaces with mean surface roughnesses of 0.13 and 0.17 nm, respectively, as revealed by atomic force microscopy (AFM). AFM images were scanned by Veeco diMultimodeV with NanoscopeV controller. The E-scanner with Appnano ACTA silicon probe scanned in tapping mode provided information of height and phase within a size of 2 micrometers. The XRR measurement was performed by the Bruker AXS Model D8 Advance. The thickness and roughness of the PS film was further confirmed by X-ray reflectivity measurement. The results were shown in **Figure S3** in the Supplementary Information.

Organic semiconductors were thermally evaporated on the substrates at 4×10^{-6} torr at a rate of 0.2 Å/s. Both source and drain electrodes were made by 20 nm of MoO_3 and 100 nm of Au. MoO_3 could enhance the hole injection efficiency in the hole transporters.[33-34] All TFT devices were bottom-gate top-contact as shown in **Figure S4**. Unless stated otherwise, the thickness of the organic layers were 100 nm. The capacitance per unit area C_i was measured by making a device with the structure SiO2/dielectric layer/Au and measured by the Hioki 3532-50 LCR HiTESTER with a two point probe. Besides TFT, the hole mobilities of some HTs were also examined by time-of-flight (TOF) technique.[35] For TOF measurement, a thick organic layer with an average thickness of 5 μm was needed for reliable measurements. Details of TOF experiments have been reported elsewhere.[35,36] In additional to TFT and TOF samples, bare organic films were grown on both SiO_2 and PS surfaces. Grazing incidence X-Ray diffraction technique (GIXRR) to examine the crystallinity of these organic films on both SiO_2 and PS surfaces. The spectra were featureless and did not reveal information on the ordering and orientations.

Acknowledgment

Support for this work under the Research Grant Council of Hong Kong under Grant No. #12201914 and #FRG2/12-13/080 is gratefully acknowledged. This work is also partially supported by the Research Grant Council of Hong Kong under Project #21201514.

Received: ((will be filled in by the editorial staff))

Revised: ((will be filled in by the editorial staff))
Published online: ((will be filled in by the editorial staff))

[1] P. Kordt, J. J. M. van der Holst, M. A. Helwi, W. Kowalsky, F. May, A. Badinski, C. Lennartz, and D. Andrienko, *Adv. Funct. Mater.* **2014**, *25*, 1955

[2] F. Guo, N. Li, V. V. Radmilovic, V. R. Radmilovic, M. Turbiez, E. Spiecker, K. Forberich, C. J. Brabec, *Energy & Environ. Science.* **2015**, *8*, 1631

[3] T. Higuchi, H. Nakanotani, C. Adachi, *Adv. Mater.* **2015**, *27*, 2019

[4] M. A. Green, K. Emery, Y. Hishikawa, W. Warta, E. D. Dunlop, *Prog. Photovolt: Res. Appl.* **2015**, 23, 1

[5] A. Zgygayevych, S. Tretiak, *Annu. Rev. Phys. Chem.* **2015**, *66*, 305

[6] M. Mizukami, S. Oku, S-I Cho, M Tatetsu, M. Abiko, M. Mamada, T. Sakanoue, Y. Suzuri, J. Kido, S. Tokito, *Electron Device Lett.* **2015**, *36*, 841

[7] S. Ho, S. Liu, Y. Chen, F. So, *Journal of Photonics for Energy.* **2015**, *5*, 057611

[8] W. Song, I. Lee, J. Y. Lee, *Adv. Mater.* **2015**, *27*, 4358

[9] J. P. Zhang, C. Wang, X. Chen, G. L. Cheng, Y. J. Qiu, M.-H. Shen, *Luminescence* **2015**, *30*, 371

[10] C. H. Y. Ho, Q. Dong, H. Yin, W. W. K. Leung, Q. Yang, H. K. H. Lee, S. W. Tsang, S. K. So, *Adv. Mater. Interfaces.* ***2015***, 1500166

[11] M. Lenes, L. J. A. Koster, V. D. Mihailetchi, P. W. M. Blom, *Appl. Phys. Lett.* ***2006***, *88*, 243502

[12] C. H. Cheung, K. C. Kwok, S. C. Tse, S. K. So, J. of Appl. Phys. **2008**, *103*, 093705

[13] H. Li, L. Duan, D. Zhang, G. Dong, J. Qian, L. Wang, Y. Qiu, *J. Phys. Chem. C* **2014**, *118*, 6052

[14] Y. Li, P. Sonar. S. P. Singh, W. Zeng, M. S. Soh, A. Dodabalapur *J. Mater. Chem.* **2011**, *21*, 10829

[15] C. Y. H. Chan, C. M. Chow, S. K. So, *Org. Electron.* **2011**, *12*, 1454

[16] A. Tsumura, H. Koezuka, T. Ando, *Appl. Phys. Lett.* **1986**, *49*, 1210

[17] G. Horowitz, R. Hajilaoui, D. Fichou, A. E. Kassmi, *J. Appl. Phys.* **1999**, *85*, 3202

[18] G. Horowitz, *J.Mater. Res.* **2004**, *19*, 1946

[19]S. W. Tsang, S. K. So, J. Appl. Phys, **2006**, *99*, 013706

[20] H. K. H. Lee, Z. Li, I. Constantinou, F. So, S. W. Tsang, S. K. So, *Adv. Energy Mater.* **2014**, *4*, 1400768

[21] D. Li, G. Dong, L. Wang, Y. Qiu, *J. Phys. Chem. C*, **2012**, *116* (8), 5235

[22] N. Matsusue, Y. Susuki and H. Naito, *Jpn. J. Appl. Phys.* **2005**, *44* (6A), 3691

[23] C. Y. H. Chan, K. K. Tsung, W. H. Choi, S. K. So, *Org. Electron.* **2013**, *14*, 1351

[24] F. Dinelli, M. Murgia, P. Levy, M. Cavalilini, F. Biscarini, *Phys. Rev. Lett.* **2004**, *92*, 116802

[25] H. Bässler, *Phys. Stat. Solid (b)*, **1993**, *175*, 15

[26] J. Veres, S. D. Ogier, S. W. Leeming, D. C. Cupertino, S. Mohialdin Khaffaf, *Adv. Funct. Mater.,* **2003**, *13*, 199

[27] H. C. F. Martens, P. W. M. Blom, H. F. M. Schoo, *Phy. Rev. B.* **2000**, *61*, 7489

[28] S. W. Tsang, M. W. Denhoff, Y. Tao, Z. H. Lu, Phys. Rev. B. **2008**, *78*, 081301

[29] S. S. Dalal, D. M. Walters, I. Lyubimov, J. J. Pablo, M. D. Ediger, *Proceedings of*

the National Academy Of Science, **2015**, *112*, 4227

[30] D. Yokoyama, *J. Mater. Chem.* **2011**, *21*, 19187

[31]J. Y. Kim, D. Yokoyama, C. Adachi, *J. Phys. Chem. C* **2012**, *116*, 8699

[32] H. T. Nicolai, M. Kuik, G. A. H. Wetzelaer, B. de Boer, C. Campbell,C. Risko, J. L. Brédas & P. W. M. Blom, *Natural Mater.* **2012**, *11*, 882

[33] Y. Zhao, J. Zhang, S. Liu, Y. Gao, X. Yang, K. S. Leck, A. P. Abiyasa, Y. Divayana, E. Mutlugun, S. T. Tan, Q. Xiong, H. V. Demir, X. W. Sun, *Org. Electron.* **2014**, *15*, 871

[34] K. K. H. Chan, S. W. Tsang, H. K. H. Lee, F. So, S. K. So, *Org. Electron,* **2012**, *13*, 850

[35] S. K. So, S. C. Tse, K. L. Tong, *J. Disp. Technol.* **2007**, *3*, 225

[36] C. H Cheung, K. K. Tsung, K. C. Kwok, S. K. So, *Appl. Phys. Lett.* **2008**, *93*, 083307

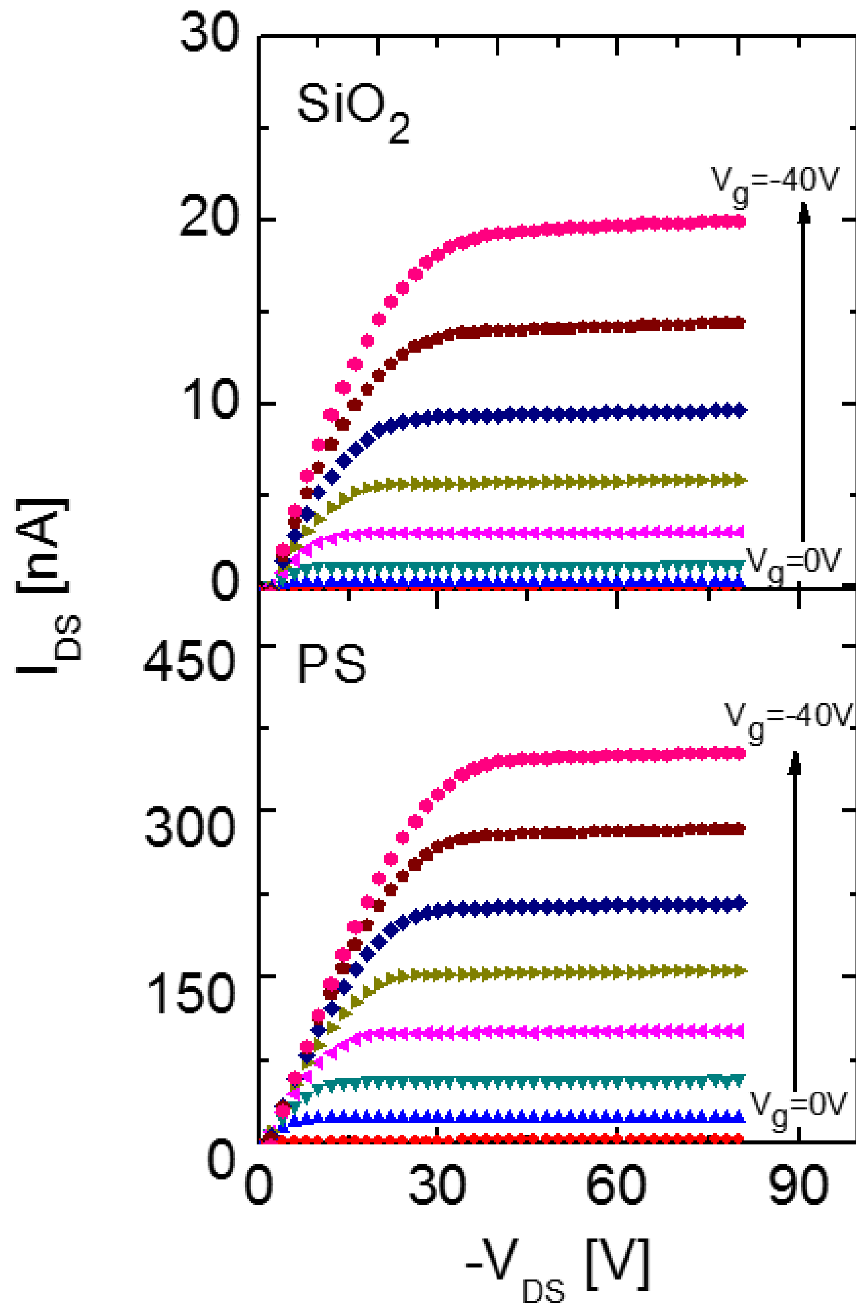

Figure 1. Typical TFT output characteristics for NPB grown on SiO_2 (top) and on PS (bottom) gate dielectric layers.

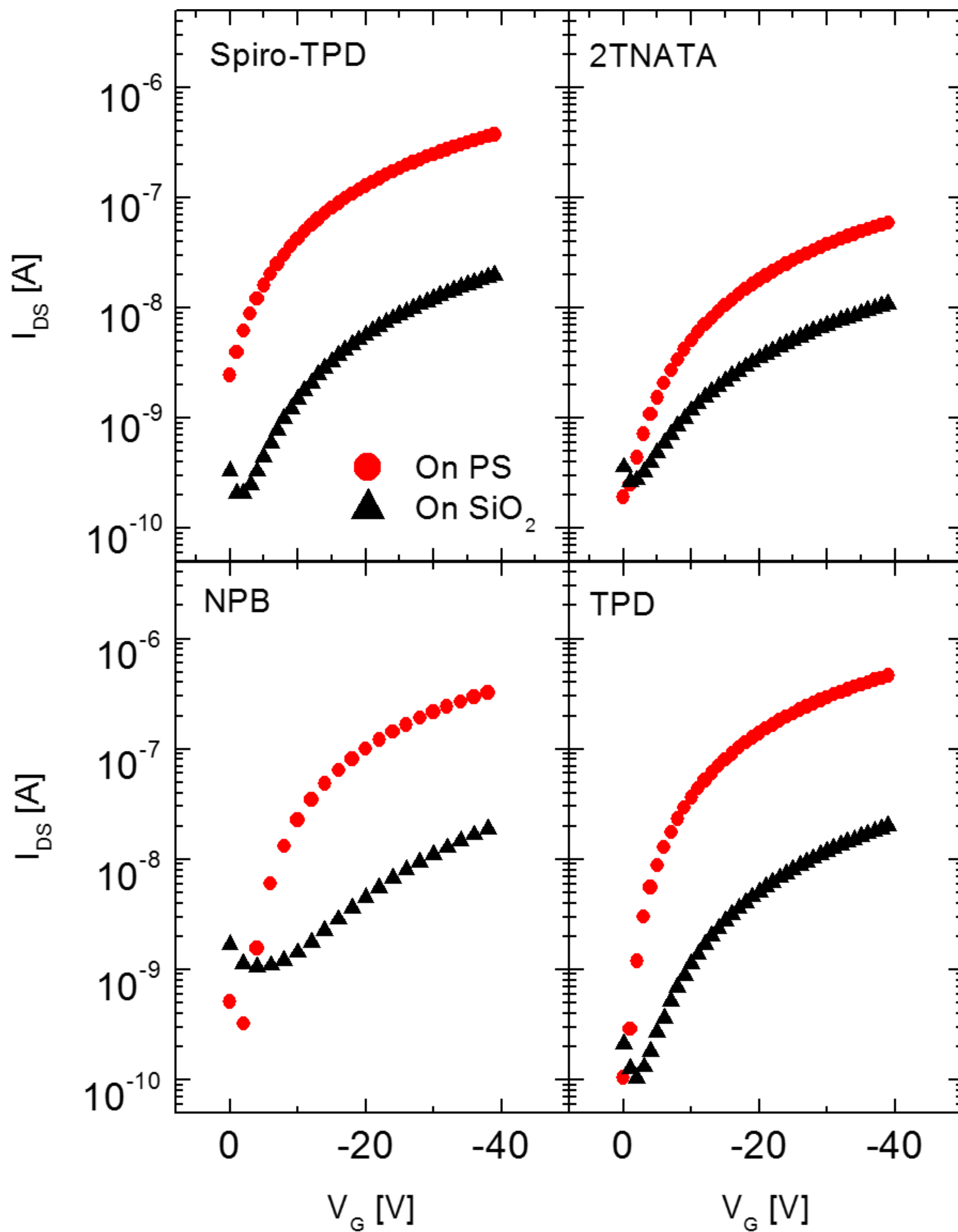

Figure 2. Transfer characteristics of four amine-based compound. All data were taken at a $V_{ds}= -60V$.

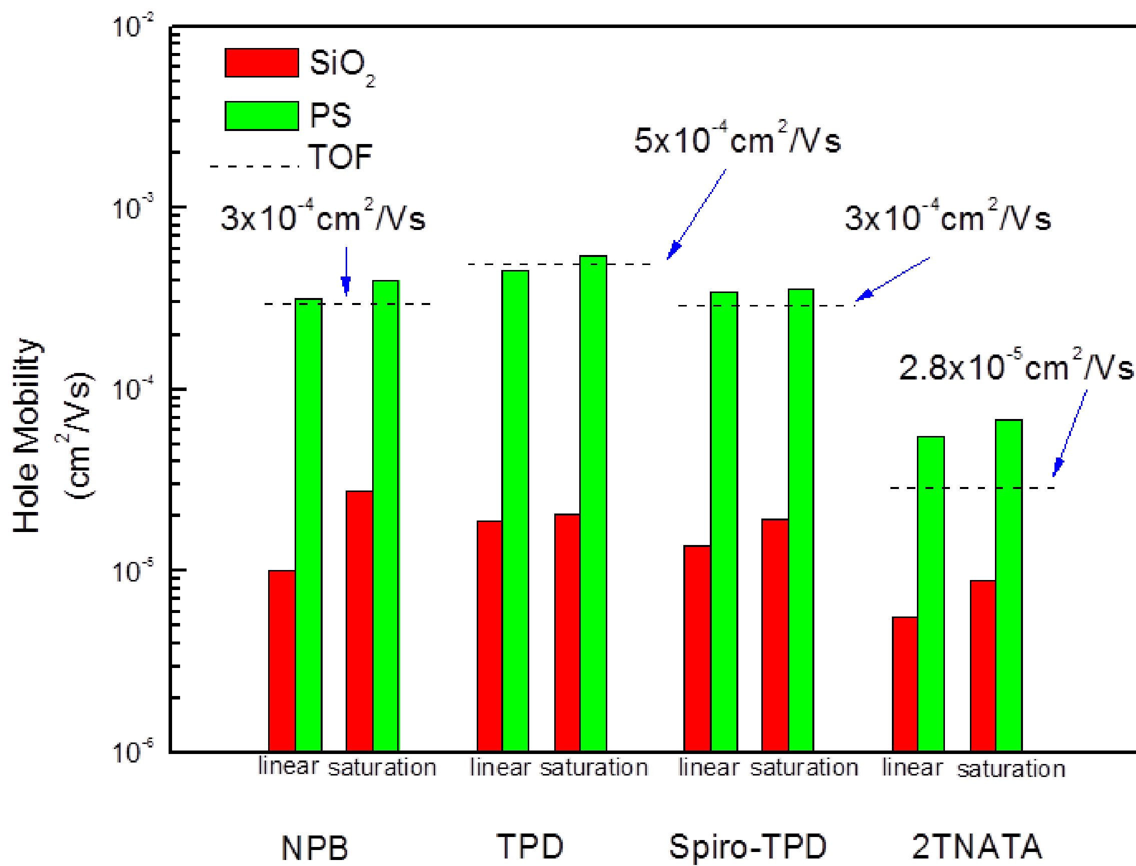

Figure 3. Bar graphs of TOF (dotted line), linear and saturation mobilities for all the amine-based compounds.

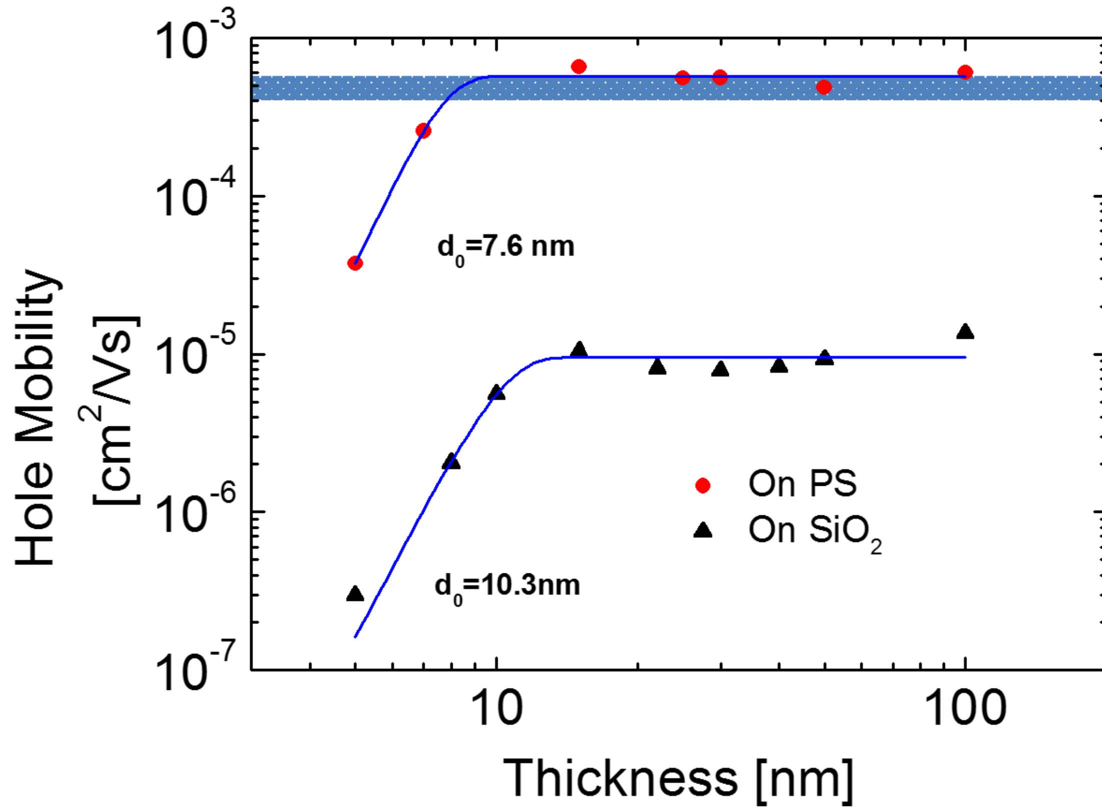

Figure 4. Thickness dependent NPB hole mobilities on SiO_2 and on PS gate dielectric layers. The solid curves are fitted curves to the experimental data using Equation 3. The horizontal band represents the range of mobilities from TOF measurements.

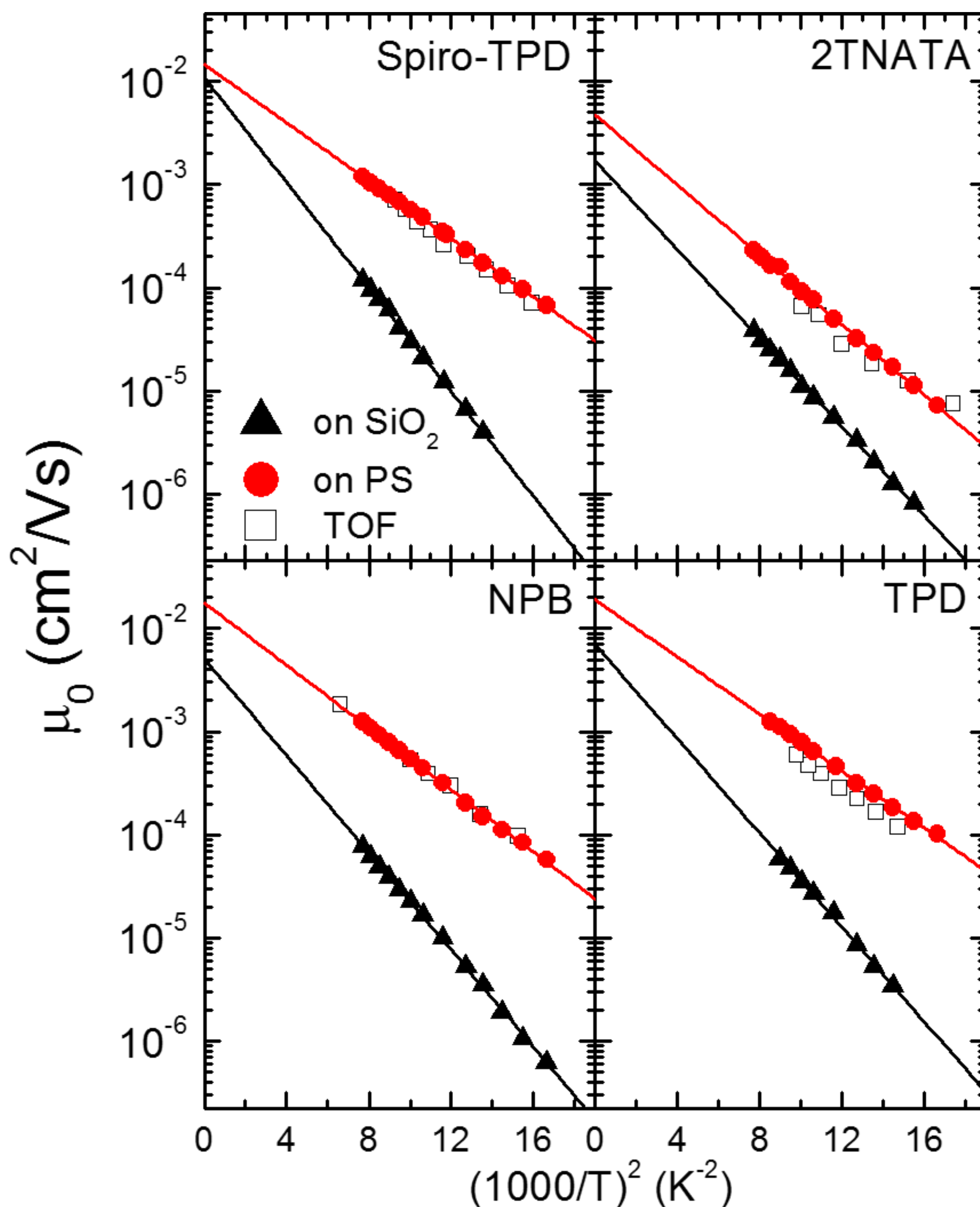

Figure 5. Temperature dependent TFT-derived mobilities data for all the four amine-based compounds analyzed by the GDM model. Black triangles and red circles represent the TFT mobility on SiO_2 and, PS respectively. Hollow squares represent the hole mobilities obtained from TOF measurements.

	σ_{TFT,SiO_2} (meV)	$\sigma_{TFT,PS}$ (meV)	σ_{TOF} (meV)	μ_{∞,SiO_2} (cm^2/Vs)	$\mu_{\infty,PS}$ (cm^2/Vs)
Spiro-TPD	98	73	75	1x10^{-2}	1.5x10^{-2}
2TNATA	91	77	71	1.7x10^{-3}	4.7x10^{-3}
NPB	95	74	76	5x10^{-3}	1.8x10^{-2}
TPD	94	71	74	7x10^{-3}	1.9x10^{-2}

Table. 1 Energetic disorders and high temperature limits of the mobility obtained from TFT and TOF techniques.

	μ_{∞,SiO_2} (cm^2/Vs)	$\mu_{\infty,PS}$ (cm^2/Vs)	a_{SiO_2} (nm)	a_{PS} (nm)
Spiro-TPD	1x10^{-2}	1.5x10^{-2}	1.04	1.03
2TNATA	1.7x10^{-3}	4.7x10^{-3}	1.87	1.70
NPB	5x10^{-3}	1.8x10^{-2}	1.20	0.93
TPD	7x10^{-3}	1.9x10^{-2}	1.14	0.92

Table 2. μ_∞ and average hopping distances of all amine compounds on PS and SiO_2 surfaces.

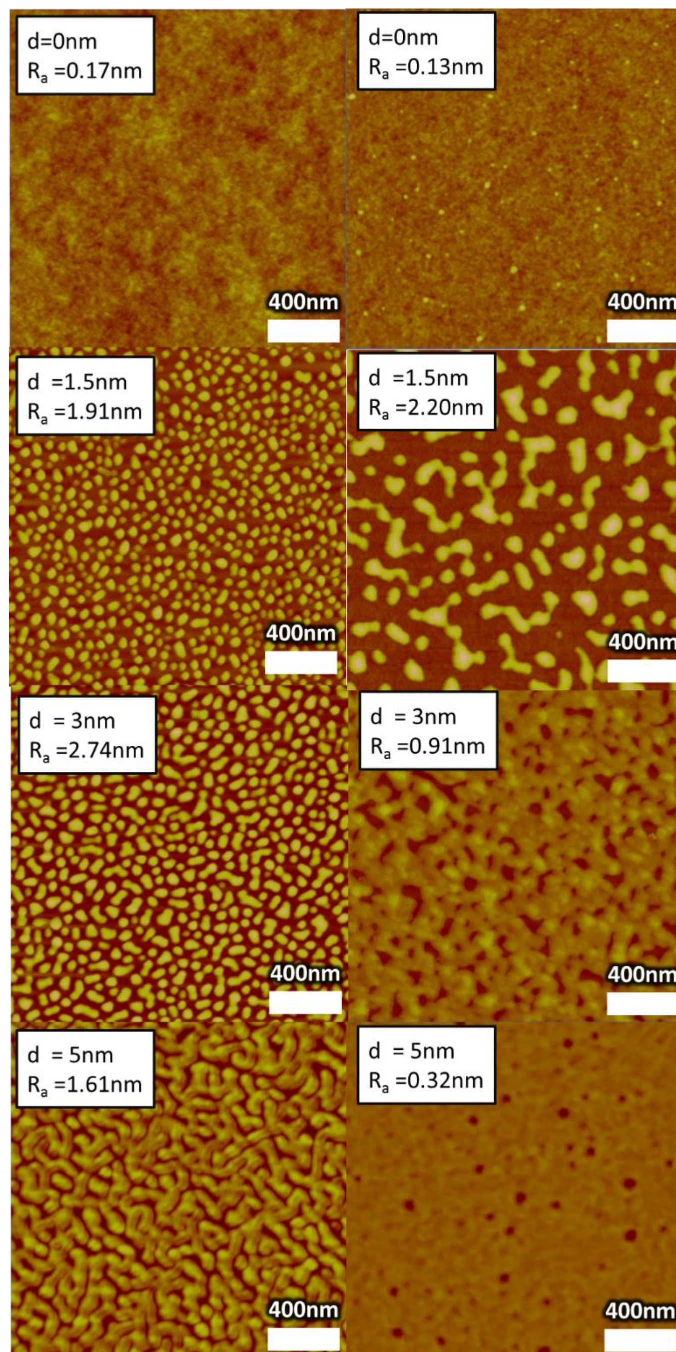

Figure 6. AFM images of NPB molecules on PS (left column) and SiO_2 (right column). Different nominal thicknesses, d and average roughness, R_a are also shown in each figure.

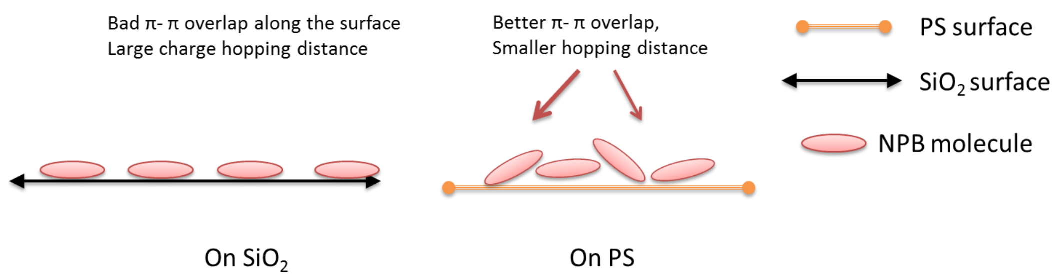

Figure 7. A model for the molecular orientations of NPB on SiO_2 and PS.

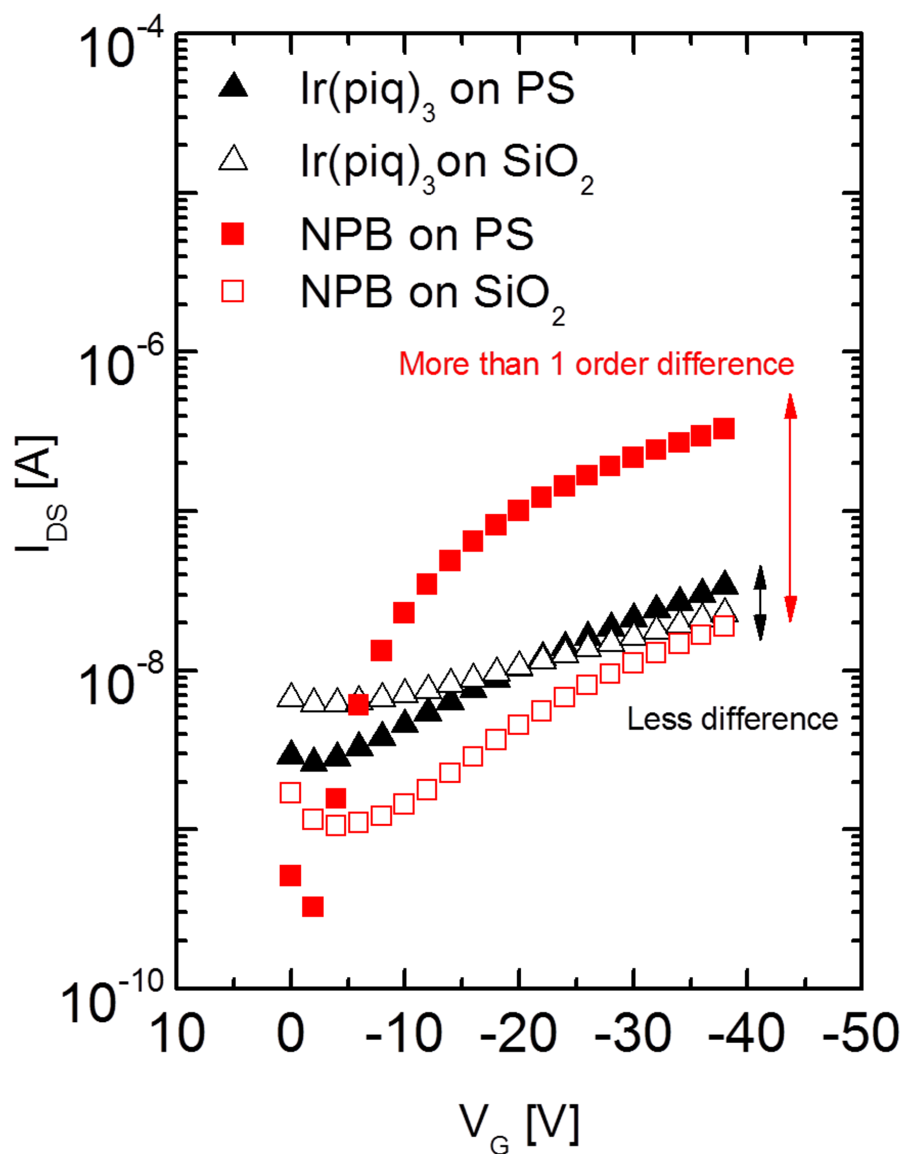

Figure 8. Transfer characteristics of $Ir(piq)_3$ and NPB on PS and SiO_2 gate dielectric layers. For $Ir(piq)_3$, the transfer cures are similar on both PS and SiO_2. For NPB, the transfer curves have more than 1 order of difference in magnitudes.

Copyright WILEY-VCH Verlag GmbH & Co. KGaA, 69469 Weinheim, Germany, 2013.

Supporting Information

Title: Probing bulk transport, interfacial disorders, and molecular orientations of amorphous semiconductors on a thin-film transistor configuration

*Wai-Yu Sit, Sin Hang Cheung, Cyrus Yiu Him Chan, Ken Ka Kin Tsung, Sai Wing Tsang, and Shu Kong So**

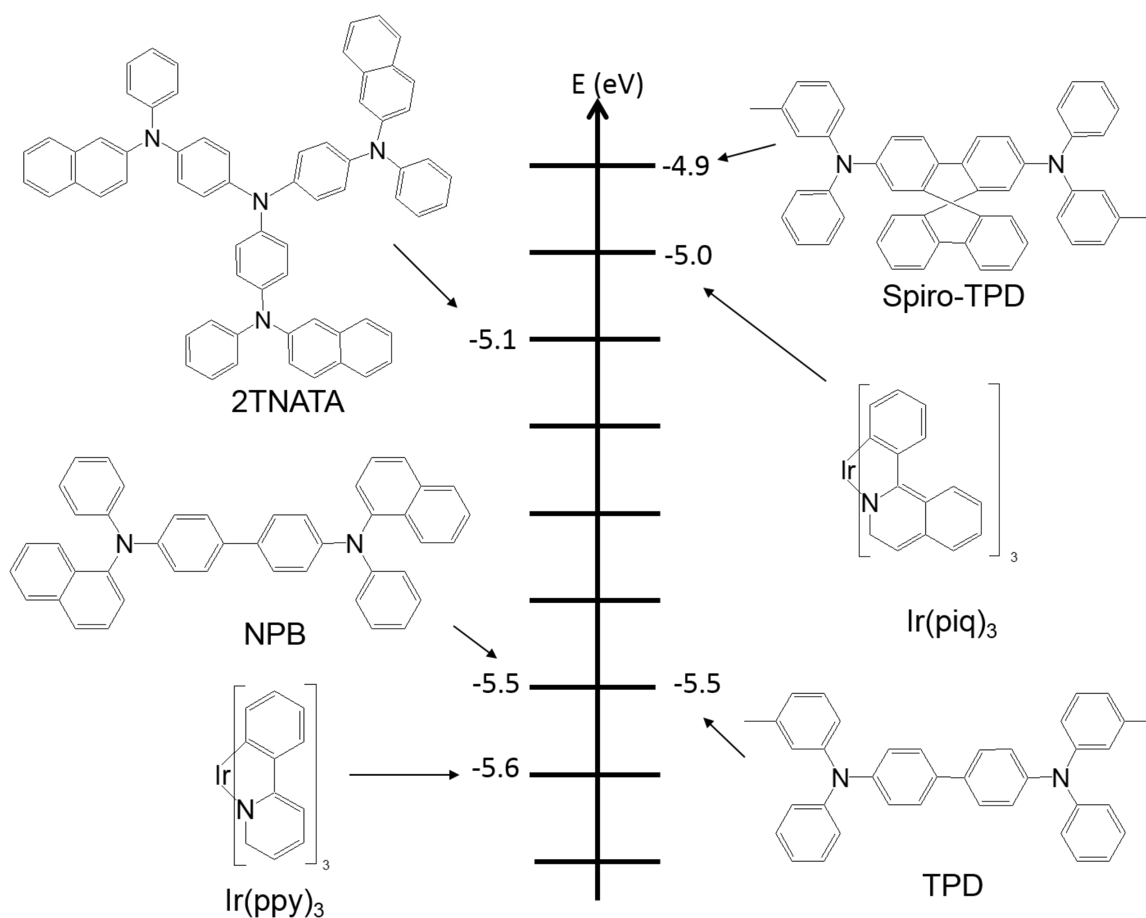

Figure S1. Chemical structures and the HOMO values of four organic amine-based hole transporters, and two iridium-based compounds, $Ir(piq)_3$, and $Ir(ppy)_3$.

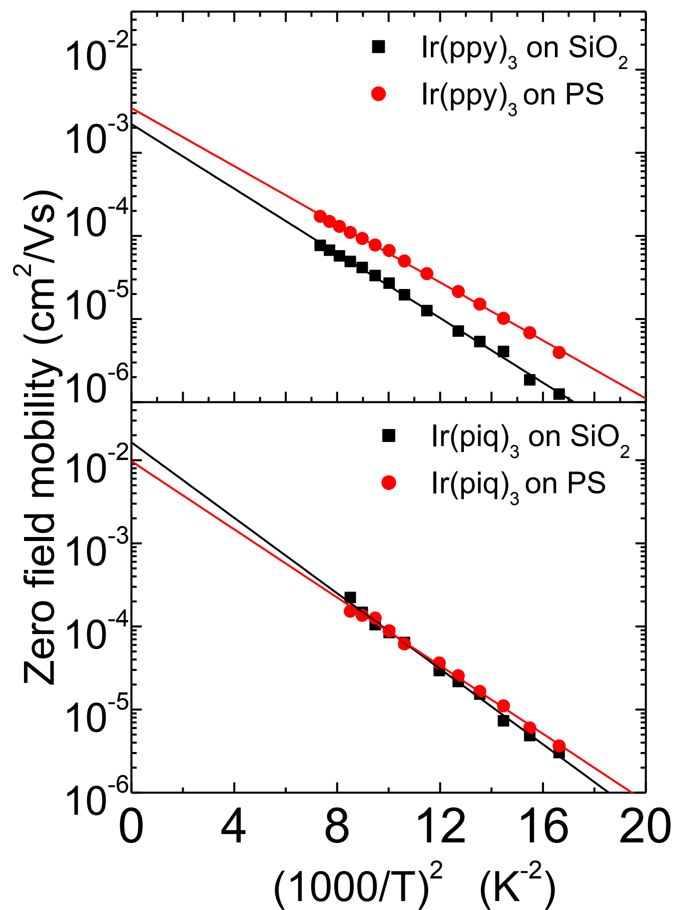

Figure S2a. Temperature dependent measurements of $Ir(ppy)_3$ and $Ir(piq)_3$ on PS and SiO_2.

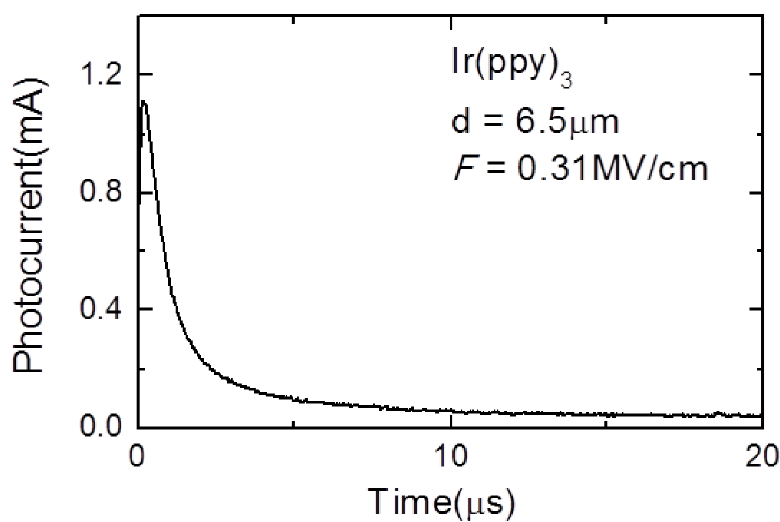

Figure S2b. Time of flight (TOF) data for $Ir(ppy)_3$.

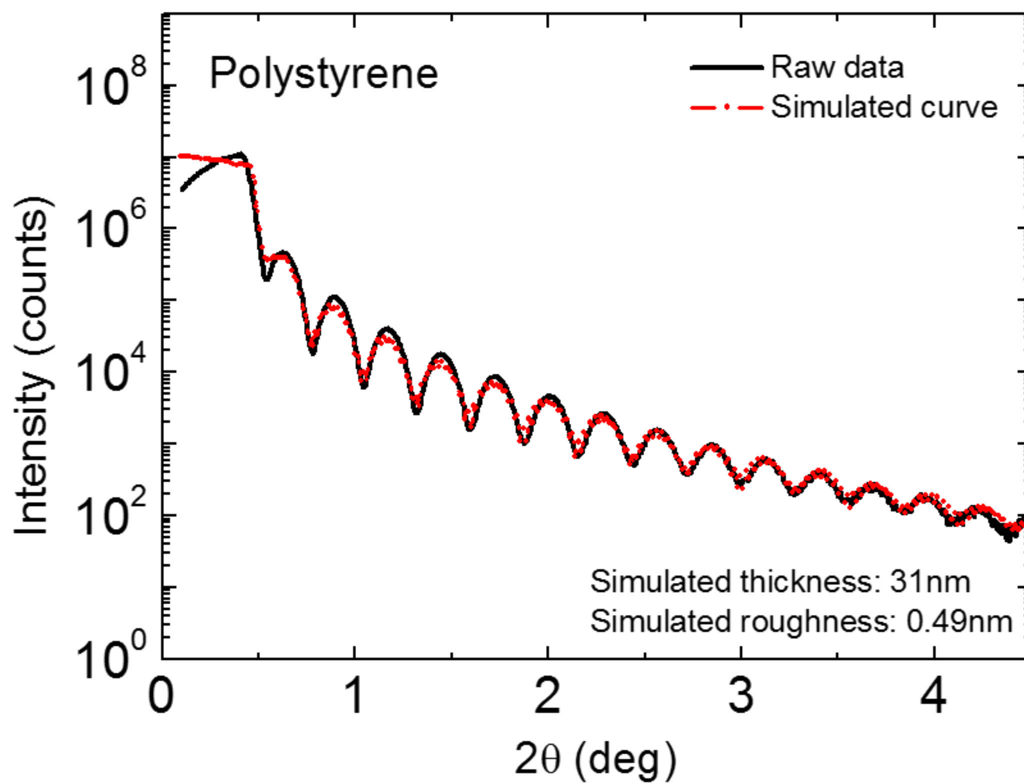

Figure S3. X-Ray reflectivity (XRR) measurements of polystyrene (PS) grown on SiO_2. The thickness and roughness of the PS overlayer can be extracted from the experimental data by simulating the experimental data as indicated.

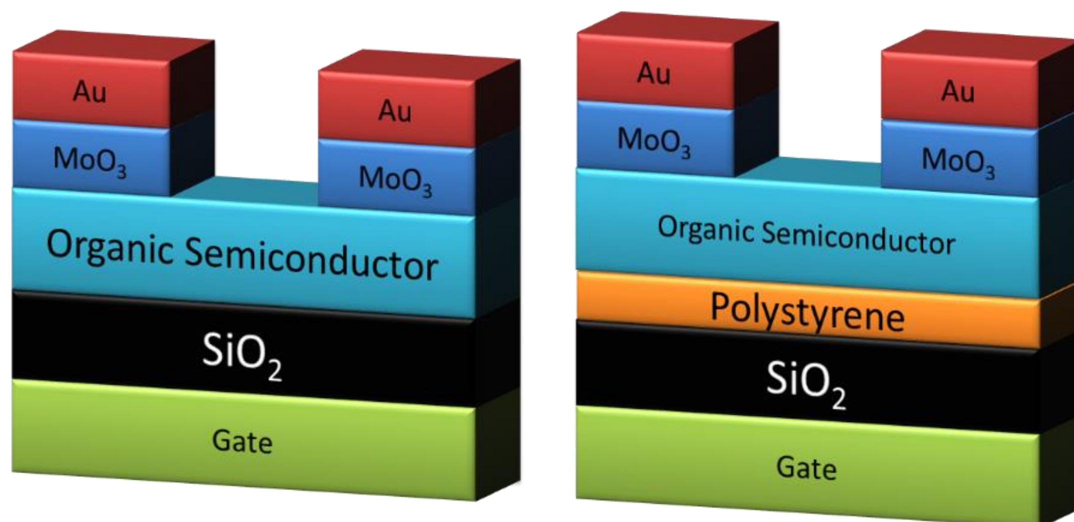

Figure S4. Bottom gate top contact TFT device structure.

	μ_{lin} (cm^2/Vs)	μ_{sat} (cm^2/Vs)	V_t (V)	On/off ratio
Spiro-TPD	3.4×10^{-4} (1.4×10^{-5})	3.5×10^{-4} (1.9×10^{-5})	4.7 (2)	1.5×10^{2} (9.6×10^{1})
2TNATA	5×10^{-5} (5.5×10^{-6})	6.6×10^{-5} (8.9×10^{-6})	2 (2.9)	3.1×10^{2} (1.1×10^{1})
NPB	3.2×10^{-4} (1×10^{-5})	3.9×10^{-4} (2.8×10^{-5})	1.3 (-5.5)	1×10^{3} (1.8×10^{1})
TPD	4.6×10^{-4} (1.8×10^{-5})	5.3×10^{-4} (2.1×10^{-5})	1.3 (-1.1)	4.4×10^{3} (1.3×10^{2})

Table S1. Device parameters of TFT using PS as gate dielectric. Values in brackets correspond to SiO_2 gate dielectric.